EUROPEAN ORGANIZATION FOR NUCLEAR RESEARCH (CERN)

CERN-EP/2002-021
March 13, 2002

Search for gauge mediated SUSY breaking topologies in e^+e^- collisions at centre–of–mass energies up to 209 GeV

The ALEPH Collaboration *)

Abstract

A total of 628 pb^{-1} of data collected with the ALEPH detector at centre-of-mass energies from 189 to 209 GeV is analysed in the search for gauge mediated SUSY breaking (GMSB) topologies. These topologies include two acoplanar photons, non-pointing single photons, acoplanar leptons, large impact parameter leptons, detached slepton decay vertices, heavy stable charged sleptons and multi-leptons plus missing energy final states. No evidence is found for new phenomena, and lower limits on masses of supersymmetric particles are derived. A scan of a minimal GMSB parameter space is performed and lower limits are set for the next-to-lightest supersymmetric particle (NLSP) mass at 54 GeV/c^2 and for the mass scale parameter Λ at 10 TeV/c^2, independently of the NLSP lifetime. Including the results from the neutral Higgs boson searches, a NLSP mass limit of 77 GeV/c^2 is obtained and values of Λ up to 16 TeV/c^2 are excluded.

(Submitted to European Physics Journal C)

*) See next pages for the list of authors

The ALEPH Collaboration

A. Heister, S. Schael

Physikalisches Institut das RWTH-Aachen, D-52056 Aachen, Germany

R. Barate, R. Brunelière, I. De Bonis, D. Decamp, C. Goy, S. Jezequel, J.-P. Lees, F. Martin, E. Merle, M.-N. Minard, B. Pietrzyk, B. Trocmé

Laboratoire de Physique des Particules (LAPP), IN^{2}P^3-CNRS, F-74019 Annecy-le-Vieux Cedex, France

G. Boix,[25] S. Bravo, M.P. Casado, M. Chmeissani, J.M. Crespo, E. Fernandez, M. Fernandez-Bosman, Ll. Garrido,[15] E. Graugés, J. Lopez, M. Martinez, G. Merino, R. Miquel,[4] Ll.M. Mir,[4] A. Pacheco, D. Paneque, H. Ruiz

Institut de Física d'Altes Energies, Universitat Autònoma de Barcelona, E-08193 Bellaterra (Barcelona), Spain[7]

A. Colaleo, D. Creanza, N. De Filippis, M. de Palma, G. Iaselli, G. Maggi, M. Maggi, S. Nuzzo, A. Ranieri, G. Raso,[24] F. Ruggieri, G. Selvaggi, L. Silvestris, P. Tempesta, A. Tricomi,[3] G. Zito

Dipartimento di Fisica, INFN Sezione di Bari, I-70126 Bari, Italy

X. Huang, J. Lin, Q. Ouyang, T. Wang, Y. Xie, R. Xu, S. Xue, J. Zhang, L. Zhang, W. Zhao

Institute of High Energy Physics, Academia Sinica, Beijing, The People's Republic of China[8]

D. Abbaneo, P. Azzurri, T. Barklow,[30] O. Buchmüller,[30] M. Cattaneo, F. Cerutti, B. Clerbaux, H. Drevermann, R.W. Forty, M. Frank, F. Gianotti, T.C. Greening,[26] J.B. Hansen, J. Harvey, D.E. Hutchcroft, P. Janot, B. Jost, M. Kado,[2] P. Mato, A. Moutoussi, F. Ranjard, L. Rolandi, D. Schlatter, G. Sguazzoni, W. Tejessy, F. Teubert, A. Valassi, I. Videau, J.J. Ward

European Laboratory for Particle Physics (CERN), CH-1211 Geneva 23, Switzerland

F. Badaud, S. Dessagne, A. Falvard,[20] D. Fayolle, P. Gay, J. Jousset, B. Michel, S. Monteil, D. Pallin, J.M. Pascolo, P. Perret

Laboratoire de Physique Corpusculaire, Université Blaise Pascal, IN^{2}P^3-CNRS, Clermont-Ferrand, F-63177 Aubière, France

J.D. Hansen, J.R. Hansen, P.H. Hansen, B.S. Nilsson

Niels Bohr Institute, 2100 Copenhagen, DK-Denmark[9]

A. Kyriakis, C. Markou, E. Simopoulou, A. Vayaki, K. Zachariadou

Nuclear Research Center Demokritos (NRCD), GR-15310 Attiki, Greece

A. Blondel,[12] J.-C. Brient, F. Machefert, A. Rougé, M. Swynghedauw, R. Tanaka H. Videau

Laboratoire de Physique Nucléaire et des Hautes Energies, Ecole Polytechnique, IN^{2}P^3-CNRS, F-91128 Palaiseau Cedex, France

V. Ciulli, E. Focardi, G. Parrini

Dipartimento di Fisica, Università di Firenze, INFN Sezione di Firenze, I-50125 Firenze, Italy

A. Antonelli, M. Antonelli, G. Bencivenni, F. Bossi, P. Campana, G. Capon, V. Chiarella, P. Laurelli, G. Mannocchi,[5] F. Murtas, G.P. Murtas, L. Passalacqua

Laboratori Nazionali dell'INFN (LNF-INFN), I-00044 Frascati, Italy

A. Halley, J. Kennedy, J.G. Lynch, P. Negus, V. O'Shea, A.S. Thompson

Department of Physics and Astronomy, University of Glasgow, Glasgow G12 8QQ,United Kingdom[10]

S. Wasserbaech

Department of Physics, Haverford College, Haverford, PA 19041-1392, U.S.A.

R. Cavanaugh,[33] S. Dhamotharan,[34] C. Geweniger, P. Hanke, V. Hepp, E.E. Kluge, G. Leibenguth, A. Putzer, H. Stenzel, K. Tittel, M. Wunsch[19]

Kirchhoff-Institut für Physik, Universität Heidelberg, D-69120 Heidelberg, Germany[16]

R. Beuselinck, W. Cameron, G. Davies, P.J. Dornan, M. Girone,[1] R.D. Hill, N. Marinelli, J. Nowell, S.A. Rutherford, J.K. Sedgbeer, J.C. Thompson,[14] R. White

Department of Physics, Imperial College, London SW7 2BZ, United Kingdom[10]

V.M. Ghete, P. Girtler, E. Kneringer, D. Kuhn, G. Rudolph

Institut für Experimentalphysik, Universität Innsbruck, A-6020 Innsbruck, Austria[18]

E. Bouhova-Thacker, C.K. Bowdery, D.P. Clarke, G. Ellis, A.J. Finch, F. Foster, G. Hughes, R.W.L. Jones, M.R. Pearson, N.A. Robertson, M. Smizanska

Department of Physics, University of Lancaster, Lancaster LA1 4YB, United Kingdom[10]

O. van der Aa, C. Delaere, V. Lemaitre

Institut de Physique Nucléaire, Département de Physique, Université Catholique de Louvain, 1348 Louvain-la-Neuve, Belgium

U. Blumenschein, F. Hölldorfer, K. Jakobs, F. Kayser, K. Kleinknecht, A.-S. Müller, G. Quast,[6] B. Renk, H.-G. Sander, S. Schmeling, H. Wachsmuth, C. Zeitnitz, T. Ziegler

Institut für Physik, Universität Mainz, D-55099 Mainz, Germany[16]

A. Bonissent, P. Coyle, C. Curtil, A. Ealet, D. Fouchez, P. Payre, A. Tilquin

Centre de Physique des Particules de Marseille, Univ Méditerranée, IN^{2}P^3-CNRS, F-13288 Marseille, France

F. Ragusa

Dipartimento di Fisica, Università di Milano e INFN Sezione di Milano, I-20133 Milano, Italy.

A. David, H. Dietl, G. Ganis,[27] K. Hüttmann, G. Lütjens, W. Männer, H.-G. Moser, R. Settles, G. Wolf

Max-Planck-Institut für Physik, Werner-Heisenberg-Institut, D-80805 München, Germany[16]

J. Boucrot, O. Callot, M. Davier, L. Duflot, J.-F. Grivaz, Ph. Heusse, A. Jacholkowska,[32] C. Loomis, L. Serin, J.-J. Veillet, J.-B. de Vivie de Régie,[28] C. Yuan

Laboratoire de l'Accélérateur Linéaire, Université de Paris-Sud, IN^{2}P^3-CNRS, F-91898 Orsay Cedex, France

G. Bagliesi, T. Boccali, L. Foà, A. Giammanco, A. Giassi, F. Ligabue, A. Messineo, F. Palla, G. Sanguinetti, A. Sciabà, R. Tenchini,[1] A. Venturi,[1] P.G. Verdini

Dipartimento di Fisica dell'Università, INFN Sezione di Pisa, e Scuola Normale Superiore, I-56010 Pisa, Italy

O. Awunor, G.A. Blair, G. Cowan, A. Garcia-Bellido, M.G. Green, L.T. Jones, T. Medcalf, A. Misiejuk, J.A. Strong, P. Teixeira-Dias

Department of Physics, Royal Holloway & Bedford New College, University of London, Egham, Surrey TW20 OEX, United Kingdom[10]

R.W. Clifft, T.R. Edgecock, P.R. Norton, I.R. Tomalin

Particle Physics Dept., Rutherford Appleton Laboratory, Chilton, Didcot, Oxon OX11 OQX, United Kingdom[10]

B. Bloch-Devaux, D. Boumediene, P. Colas, B. Fabbro, E. Lançon, M.-C. Lemaire, E. Locci, P. Perez, J. Rander, J.-F. Renardy, A. Rosowsky, P. Seager,[13] A. Trabelsi,[21] B. Tuchming, B. Vallage

CEA, DAPNIA/Service de Physique des Particules, CE-Saclay, F-91191 Gif-sur-Yvette Cedex, France[17]

N. Konstantinidis, A.M. Litke, G. Taylor

Institute for Particle Physics, University of California at Santa Cruz, Santa Cruz, CA 95064, USA[22]

C.N. Booth, S. Cartwright, F. Combley,[31] P.N. Hodgson, M. Lehto, L.F. Thompson

Department of Physics, University of Sheffield, Sheffield S3 7RH, United Kingdom[10]

K. Affholderbach,[23] A. Böhrer, S. Brandt, C. Grupen, J. Hess, A. Ngac, G. Prange, U. Sieler

Fachbereich Physik, Universität Siegen, D-57068 Siegen, Germany[16]

C. Borean, G. Giannini

Dipartimento di Fisica, Università di Trieste e INFN Sezione di Trieste, I-34127 Trieste, Italy

H. He, J. Putz, J. Rothberg

Experimental Elementary Particle Physics, University of Washington, Seattle, WA 98195 U.S.A.

S.R. Armstrong, K. Berkelman, K. Cranmer, D.P.S. Ferguson, Y. Gao,[29] S. González, O.J. Hayes, H. Hu, S. Jin, J. Kile, P.A. McNamara III, J. Nielsen, Y.B. Pan, J.H. von Wimmersperg-Toeller, W. Wiedenmann, J. Wu, Sau Lan Wu, X. Wu, G. Zobernig

Department of Physics, University of Wisconsin, Madison, WI 53706, USA[11]

G. Dissertori

Institute for Particle Physics, ETH Hönggerberg, 8093 Zürich, Switzerland.

[1]Also at CERN, 1211 Geneva 23, Switzerland.
[2]Now at Fermilab, PO Box 500, MS 352, Batavia, IL 60510, USA
[3]Also at Dipartimento di Fisica di Catania and INFN Sezione di Catania, 95129 Catania, Italy.
[4]Now at LBNL, Berkeley, CA 94720, U.S.A.
[5]Also Istituto di Cosmo-Geofisica del C.N.R., Torino, Italy.
[6]Now at Institut für Experimentelle Kernphysik, Universität Karlsruhe, 76128 Karlsruhe, Germany.
[7]Supported by CICYT, Spain.
[8]Supported by the National Science Foundation of China.
[9]Supported by the Danish Natural Science Research Council.
[10]Supported by the UK Particle Physics and Astronomy Research Council.
[11]Supported by the US Department of Energy, grant DE-FG0295-ER40896.
[12]Now at Departement de Physique Corpusculaire, Université de Genève, 1211 Genève 4, Switzerland.
[13]Supported by the Commission of the European Communities, contract ERBFMBICT982874.
[14]Supported by the Leverhulme Trust.
[15]Permanent address: Universitat de Barcelona, 08208 Barcelona, Spain.
[16]Supported by Bundesministerium für Bildung und Forschung, Germany.
[17]Supported by the Direction des Sciences de la Matière, C.E.A.
[18]Supported by the Austrian Ministry for Science and Transport.
[19]Now at SAP AG, 69185 Walldorf, Germany
[20]Now at Groupe d' Astroparticules de Montpellier, Université de Montpellier II, 34095 Montpellier, France.
[21]Now at Département de Physique, Faculté des Sciences de Tunis, 1060 Le Belvédère, Tunisia.
[22]Supported by the US Department of Energy, grant DE-FG03-92ER40689.
[23]Now at Skyguide, Swissair Navigation Services, Geneva, Switzerland.
[24]Also at Dipartimento di Fisica e Tecnologie Relative, Università di Palermo, Palermo, Italy.
[25]Now at McKinsey and Compagny, Avenue Louis Casal 18, 1203 Geneva, Switzerland.
[26]Now at Honeywell, Phoenix AZ, U.S.A.
[27]Now at INFN Sezione di Roma II, Dipartimento di Fisica, Università di Roma Tor Vergata, 00133 Roma, Italy.
[28]Now at Centre de Physique des Particules de Marseille, Univ Méditerranée, F-13288 Marseille, France.
[29]Also at Department of Physics, Tsinghua University, Beijing, The People's Republic of China.
[30]Now at SLAC, Stanford, CA 94309, U.S.A.
[31]Deceased.
[32]Also at Groupe d' Astroparticules de Montpellier, Université de Montpellier II, 34095 Montpellier, France.
[33]Now at University of Florida, Department of Physics, Gainesville, Florida 32611-8440, USA
[34]Now at BNP Paribas, 60325 Frankfurt am Mainz, Germany

1 Introduction

If supersymmetry (SUSY) were an exact symmetry, the new SUSY particles would be degenerate in mass with their Standard Model (SM) partners. As no experimental evidence has been found to prove the existence of SUSY particles, supersymmetry must be a broken symmetry. In Gauge Mediated SUSY Breaking (GMSB) models, supersymmetry is broken at a high energy scale in a hidden or "secluded" sector and is then propagated down to the visible sector via the SM gauge interactions [1]. The main motivation for GMSB models lies in the fact that they can easily cope with the experimental absence of flavour changing neutral currents (FCNC). Gauge interactions are flavour blind and the scale at which SUSY breaking is mediated is expected to be well below the scale at which flavour symmetry should be broken.

From the phenomenological point of view the main difference with respect to gravity mediated SUSY breaking models (SUGRA) [2] is that in GMSB the lightest supersymmetric particle (LSP) is the gravitino ($\tilde{\mathrm{G}}$) which couples very weakly to the other particles. Assuming R-parity conservation, SUSY particles are pair produced in $\mathrm{e^+e^-}$ collisions and subsequently decay to their SM partner plus gravitinos. Another important characteristic of these models is that the next-to-lightest supersymmetric particle (NLSP) is, in general, either the lightest neutralino χ or the sleptons $\tilde{\ell}$. In GMSB models a non-negligible mixing between $\tilde{\tau}_{\mathrm{L}}$ and $\tilde{\tau}_{\mathrm{R}}$ states is expected for moderate and large values of $\tan\beta$ (the ratio of the vacuum expectation values of the two Higgs doublets) or large values of $|\mu|$ (the Higgs mixing mass term). If the stau mixing is large, the lightest stau $\tilde{\tau}_1$ becomes lighter than the other sleptons, and also possibly lighter than the neutralino, being then the only NLSP.

The lifetime of the NLSP depends on the gravitino mass (or equivalently on the SUSY breaking scale $\sqrt{F}$ which is proportional to it) [1]:

$$c\tau_{\mathrm{NLSP}} \approx \frac{0.01}{\kappa_\gamma}\left(\frac{100\,\mathrm{GeV}}{m_{\mathrm{NLSP}}}\right)^5\left(\frac{m_{\tilde{\mathrm{G}}}}{2.4\,\mathrm{eV}}\right)^2\mathrm{cm} \qquad (1)$$

where κ_γ is the bino component of the χ, and $\kappa_\gamma = 1$ for a $\tilde{\ell}$ NLSP. When cosmological considerations are taken into account, an upper limit is placed on the gravitino mass [3]: $m_{\tilde{\mathrm{G}}} \lesssim 1\,\mathrm{keV}/c^2$ ($\sqrt{F} \lesssim 2000\,\mathrm{TeV}$). Thus the gravitino mass can range from $\mathcal{O}(10^{-2})\,\mathrm{eV}/c^2$ to $1\,\mathrm{keV}/c^2$, which practically implies that any NLSP decay length is allowed. For this reason topological searches able to identify long-lived or even stable NLSP's have been developed by the ALEPH collaboration [4, 5, 6].

A previous compilation of all GMSB searches carried out by ALEPH exists with data at $\sqrt{s} = 189\,\mathrm{GeV}$ [7]. In this paper the results of the GMSB searches for all data collected at $\sqrt{s}$ up to 209 GeV are summarised. Other LEP and Tevatron experiments have reported their results in Refs. [8, 9, 10].

The organisation of this paper is the following. A brief description of the ALEPH detector is presented in Section 2. In Section 3, the experimental topologies are reviewed and limits on sparticle masses are reported. An update on four-lepton final states and the new selection for four-lepton final states when sleptons have lifetime are described in Section 3.3. In Section 4 the scan on a minimal set of GMSB parameters is presented. The sensitivity of these parameters to the different search exclusions is analysed and lower limits on the NLSP mass and the mass scale parameter Λ are derived.

2 The ALEPH detector and data samples

A detailed description of the ALEPH detector can be found in Ref. [11], and an account of its performance as well as a description of the standard analysis algorithms can be found in Ref. [12]. Only a brief overview is given here.

Charged particle tracks are measured by a silicon vertex detector (VDET), a multiwire drift chamber (ITC) and a time projection chamber (TPC). The VDET has a length of approximately 40 cm with two concentric layers of silicon wafers at average radii of 6.5 and 11.3 cm. The ITC consists of eight drift chamber layers of 2 m length between an inner radius of 16 cm and an outer radius of 26 cm. The TPC measures up to 21 space points in the radial range from 30 cm to 180 cm and has an overall length of 4.4 m. These detectors are immersed in an axial magnetic field of 1.5 T and together achieve a transverse momentum resolution $\sigma(p_{\mathrm{T}})/p_{\mathrm{T}} = 0.0006 p_{\mathrm{T}} \oplus 0.005$ (p_{T} in GeV/c). The TPC also provides up to 338 measurements of the ionisation energy loss. It is surrounded by the electromagnetic calorimeter (ECAL), which covers the angular range $|\cos\theta| < 0.98$. The ECAL is finely segmented in projective towers of approximately 0.9° by 0.9° which are read out in three segments of depth. The energy resolution is $\sigma(E)/E = 0.18/\sqrt{E} + 0.009$ (E in GeV). The iron return yoke is instrumented with streamer tubes acting as a hadron calorimeter (HCAL) and covers polar angles down to 110 mrad. Surrounding the HCAL are two additional double layers of streamer tubes called muon chambers. The luminosity monitors (LCAL and SICAL) extend the calorimetric coverage down to polar angles of 34 mrad.

Using the energy flow algorithm described in Ref. [12], the measurements of the tracking detectors and the calorimeters are combined into "objects" classified as charged particles, photons, and neutral hadrons. A *good track* is defined as a charged particle track originating from the interaction region (with transverse impact parameter $|d_0| < 1$ cm and longitudinal impact parameter $|z_0| < 5$ cm), having at least four TPC hits, a transverse momentum greater than 200 MeV/c and a minimum polar angle of 18.2°. In order to get the correct charged multiplicity, photon conversions are reconstructed with a pair-finding algorithm [12]. Electrons are identified by comparing the energy deposit in ECAL to the momentum measured in the tracking system, by using the shower profile in the electromagnetic calorimeter and by the measurement of the specific ionisation in the TPC. The tagging of muons makes use of the hit patterns in HCAL and the muon chambers.

The data samples used in this paper, collected by the ALEPH detector from 1998 to 2000, are given in Table 1. All selections were developed using Monte Carlo techniques. Simulated samples corresponding to at least ten times the collected luminosity of all major background processes have been generated. A detailed list of the Monte Carlo generators used can be found in Refs. [13, 14]. Signal samples were simulated with `SUSYGEN` [15]. The position of the

Table 1: Average centre-of-mass energy and corresponding luminosities of the analysed data sample.

Year	1998	1999				2000	
$\langle\sqrt{s}\rangle$ (GeV)	188.6	191.6	195.5	199.5	201.6	205.0	206.7
$\int \mathcal{L}\mathrm{dt}$ (pb^{-1})	173.6	28.9	79.9	87.0	44.4	79.5	134.3

most important cuts was determined using the $\bar{N}_{95}$ prescription [16], which corresponds to the minimisation of the expected 95% confidence level upper limit on the number of signal events, under the hypothesis that no signal is present in the data.

3 Review of experimental topologies and results

The nature of the NLSP determines the final state topologies to be studied in GMSB models. All the relevant searches according to the NLSP type and lifetime are listed in Table 2.

Table 2: Final state topologies studied in the different GMSB scenarios.

NLSP	Production	Decay mode	Decay length	Expected topology
χ	$e^+e^- \to \chi\chi$	$\chi \to \gamma\tilde{G}$	$\lambda \ll \ell_{\rm detector}$	Acoplanar photons
			$\lambda \sim \ell_{\rm detector}$	Non-pointing photon
			$\lambda \gg \ell_{\rm detector}$	[Indirect search]
$\tilde{\ell}$	$e^+e^- \to \tilde{\ell}\tilde{\ell}$	$\tilde{\ell} \to \ell\tilde{G}$	$\lambda \ll \ell_{\rm detector}$	Acoplanar leptons
			$\lambda \sim \ell_{\rm detector}$	Kinks and large impact parameters
			$\lambda \gg \ell_{\rm detector}$	Heavy stable charged particles
$\tilde{\ell}$	$e^+e^- \to \chi\chi$	$\chi \to \ell\tilde{\ell} \to \ell\ell\tilde{G}$	$\lambda \ll \ell_{\rm detector}$	Four leptons
			$\lambda \sim \ell_{\rm detector}$	Four leptons with lifetime
			$\lambda \gg \ell_{\rm detector}$	[Not covered here]

A detailed description of the selections optimised at 189 GeV can be found in Ref. [7]. The same selections are applied here with cut values suitably adjusted to take into account the beam energy and luminosity increases. Only the four-lepton selections, detailed in Section 3.3, and the acoplanar lepton selection, recently updated in Ref. [13], have been modified.

3.1 Neutralino NLSP

In the χ NLSP scenario, all supersymmetric decay chains will terminate in $\chi \to \tilde{G}\gamma$. Searches for pair production of neutralinos decaying promptly and neutralinos with intermediate lifetime were described in Ref. [7] and updated in Ref. [14]. For short neutralino lifetimes, the resulting experimental signature is a pair of energetic acoplanar photons. When the updated analysis is applied to the 189–209 GeV data sample, four candidate events are found with 4.9 events expected from background processes. For intermediate χ lifetimes, one neutralino may decay before reaching the electromagnetic calorimeter, while the other decays outside the detector. This scenario results in a topology where the only visible energy originates from a single photon which does not point to the interaction vertex. Two non-pointing photon events are found in the data sample and 1.0 are expected. Systematic errors have been evaluated and included in the results as in Ref. [7].

For long χ NLSP decay lengths ($\lambda \gg \ell_{\rm detector}$) the neutralino becomes invisible and only indirect exclusions are possible. The relationship between the χ mass and the slepton and

chargino masses can be exploited to put indirect limits on the χ mass using the ALEPH results on slepton [13] and chargino [17] searches performed within the SUGRA framework.

The combination of all these analyses allows the exclusion of neutralino masses as a function of the neutralino decay length. An example for a particular region in the GMSB parameter space is shown in Fig. 1.

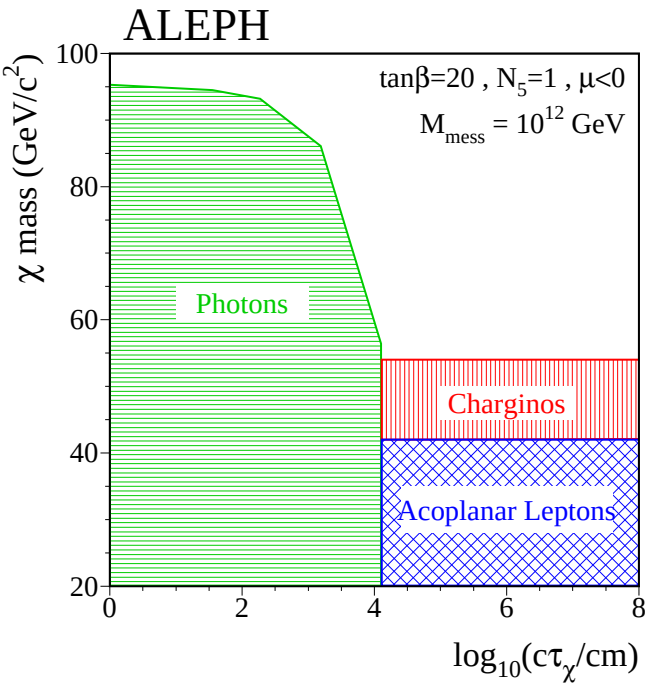

Figure 1: Excluded neutralino mass at 95% confidence level as a function of its lifetime in the neutralino NLSP scenario. The excluded areas are obtained by the scan described in Section 4 for negative μ, $N_5 = 1$, $M_{\rm mess} = 10^{12}\,{\rm GeV}/c^2$, $\tan\beta = 20$ and any Λ. The short and medium lifetime cases, when at least one χ decays inside the detector, are covered by the acoplanar photons and non-pointing photon searches. For long-lived neutralinos the gravity mediated searches for charginos and sleptons are used.

3.2 Slepton NLSP direct decay

In the case of a slepton NLSP, the pair-production process $e^+e^- \to \tilde{\ell}\tilde{\ell}$ is expected to be the main experimental signature. The signal final state topology depends strongly on the slepton lifetime. Four different analyses are performed, each corresponding to a specific range of mean decay length. These searches were described in Ref. [6] and updated in Ref. [7].

If the $\tilde{\ell}$ has a short decay length, of the order of a few mm or less, the final state topology will be a pair of acoplanar leptons and missing energy, carried away by the two gravitinos. This final state is studied in gravity mediated models [13], where a neutralino of almost zero

mass plays the role of the gravitino in GMSB. Therefore, the results obtained for a massless neutralino are used.

Sleptons with intermediate lifetime, which decay inside the detector, may show two possible signatures: large impact parameter and kinked tracks. If the slepton decays before the TPC, between $\sim$1 cm and 40 cm, the slepton track will not be reconstructed and the final lepton track will have a large impact parameter. If the slepton decays within the TPC volume, the signature is then characterised by a kinked track. Two different selections are therefore applied to the intermediate slepton lifetime case. One event is found with 1.1 events expected from SM processes.

Finally, long-lived sleptons can be detected from their anomalous specific ionisation in the TPC. The search for heavy stable charged particles selected one candidate event, while 2.3 are expected from background processes.

The effect of systematic uncertainties on kinematic cuts has been studied as in Ref. [7] and limits are derived reducing the efficiency by a total systematic error of 5%. When all four independent selections are combined, the 95% confidence level lower limits on the right-slepton masses, independent of lifetime, are set at 83, 88 and 77 GeV/c^2 for selectron, smuon and stau, respectively. The selectron mass limit is obtained neglecting the t-channel exchange contribution to the production cross section. The stau mass limit as a function of lifetime is plotted in Fig. 2.

3.3 Slepton NLSP cascade decays

In the $\tilde{\ell}$ NLSP scenario, if the neutralino pair production is kinematically accessible, the process $\mathrm{e^+e^-} \to \chi\chi \to \ell\tilde{\ell}\,\ell\tilde{\ell} \to \ell\ell\tilde{\mathrm{G}}\,\ell\ell\tilde{\mathrm{G}}$ may provide a very distinctive discovery signal. This cascade decay can increase the sensitivity to GMSB signatures in some region of the parameter space. This process benefits from quite a large cross section (the χ is expected to be mainly bino and the $\tilde{\mathrm{e}}_\mathrm{R}$ is expected to be light) and from a clear experimental signature. Four leptons are produced in the final state (two could be soft if the χ-$\tilde{\ell}$ mass difference is small) and in half of the cases the two most energetic leptons have the same charge (χ are Majorana particles).

Depending on the flavour of the slepton in $\chi \to \ell\tilde{\ell}$ decays, there are six possible topologies, labelled $\tilde{\mathrm{e}}\tilde{\mathrm{e}}$, $\tilde{\mu}\tilde{\mu}$, $\tilde{\tau}\tilde{\tau}$, $\tilde{\mathrm{e}}\tilde{\mu}$, $\tilde{\mathrm{e}}\tilde{\tau}$ and $\tilde{\mu}\tilde{\tau}$ in the case of slepton co-NLSP. In the case of stau NLSP only the $\tilde{\tau}\tilde{\tau}$ topology is relevant.

3.3.1 Prompt decays

Searches for the cascade topologies with negligible lifetime have already been performed by ALEPH at a centre-of-mass energy of 189 GeV [7]. The selection cuts are revisited in this paper to improve the signal efficiencies and account for the increase in centre-of-mass energy and luminosity. The revised cuts described in Appendix A are also applied to the data collected at 189 GeV and improve the signal efficiency up to 10%.

The main systematic uncertainties on the background and signal expectations come from the number of generated events in the simulated samples (up to 4%). A total systematic

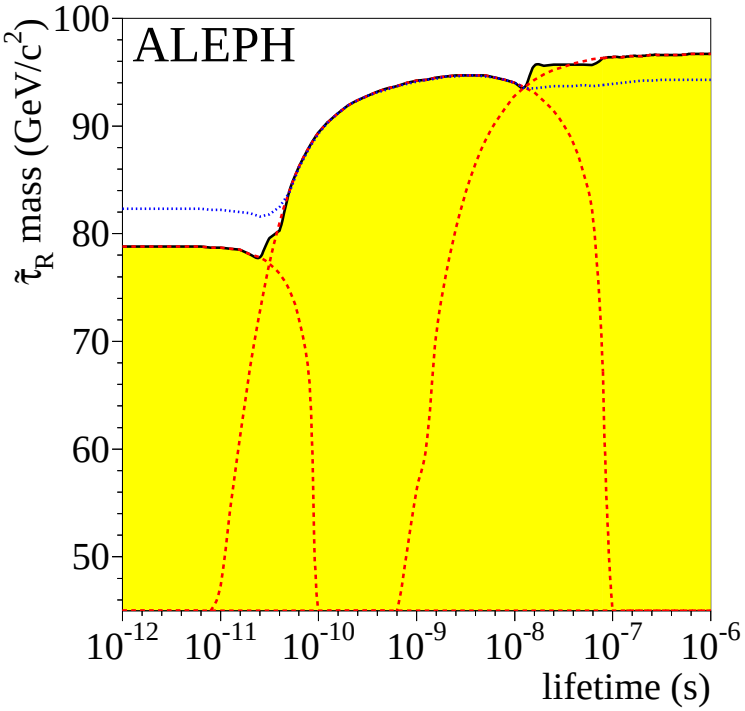

Figure 2: Excluded $\tilde{\tau}_R$ mass at 95% C.L. as a function of its lifetime (shaded area) from direct searches. Dashed curves give the limits from the different topologies. The search for acoplanar leptons covers the case of small lifetimes, searches for tracks with large impact parameter and for kinks are used in the intermediate range, whereas for very large lifetimes a search for heavy stable charged particles is performed. The dotted curve gives the expected limit.

uncertainty of 2% is evaluated for the variables involved in the selection. To derive the results, the selection efficiency has been reduced by 4%.

The efficiency of the cuts on the signal samples was found to be in the range 65–85% for χ-$\tilde{\ell}$ mass differences greater than $3\,\mathrm{GeV}/c^2$ in the case of final states not involving tau leptons and in the range 40–65% for χ-$\tilde{\ell}$ mass differences greater than $5\,\mathrm{GeV}/c^2$ in the case of final states with tau leptons. The selection efficiencies for the six topologies are shown in Fig. 3a.

The numbers of background events expected from Standard Model processes and of events observed in the data are given in Table 3. The largest background contributions are from WW and $\tau\tau(\gamma)$ events.

3.3.2 Short and long decays

A new analysis has been developed for the case of observable slepton decay length, based on the experimental signatures of leptons with large impact parameter and track kinks. Searches were developed for each of the six channels, consisting of loose cuts on global event variables, which cause very little signal rejection, and of more stringent cuts on individual track properties. The latter are intended to select the tracks that come from the decay of the long-lived sleptons. For

Table 3: Expected Standard Model background and selected candidates for the various cascade topologies in the case of negligible slepton lifetime.

Energy	$\tilde{e}\tilde{e}$		$\tilde{\mu}\tilde{\mu}$		$\tilde{e}\tilde{\mu}$		$\tilde{\tau}\tilde{\tau}$		$\tilde{e}\tilde{\tau}$		$\tilde{\mu}\tilde{\tau}$	
(GeV)	exp	obs	exp	obs	exp	obs	exp	obs	exp	obs	exp	obs
188.6	1.33	2	0.12	1	0.98	1	5.23	4	1.34	2	1.77	0
191.6	0.31	1	0.02	0	0.29	0	1.17	1	0.33	1	0.29	1
195.5	1.05	2	0.07	0	0.41	0	1.84	7	0.72	0	0.61	0
199.5	0.88	1	0.04	0	0.69	0	2.19	2	0.85	2	0.86	1
201.6	0.27	0	0.03	0	0.17	1	0.97	3	0.30	0	0.33	0
205.0	0.51	0	0.07	0	0.41	0	1.96	1	0.72	0	0.62	1
206.7	0.80	0	0.09	0	0.70	0	3.13	4	1.26	3	1.24	2
Total	5.15	6	0.44	1	3.65	2	16.49	22	5.52	8	5.72	5

Table 4: Summary of results for the case of observable slepton decay length in cascade decays: the numbers of observed candidate events passing at least one topology and of expected background events for both decay length selections.

Energy	Short decay length		Long decay length	
(GeV)	expected	observed	expected	observed
188.6	1.39	0	0.51	1
191.6	0.24	2	0.08	1
195.5	0.66	1	0.20	1
199.5	0.73	0	0.20	0
201.6	0.38	0	0.10	0
205.0	0.69	0	0.16	0
206.7	1.16	2	0.26	1
Total	5.25	5	1.51	4

each topology, two independent selections were designed to ensure good sensitivity to the signal both for short ($\sim$1 cm) and long ($\sim$1 m) decay lengths. Further details are given in Appendix B.

Because the searches in all topologies focus primarily on selecting tracks with large d_0, there is a large overlap in their acceptances, and so candidate events tend to be selected more than once. The "efficiency" (the probability for a signal event to be selected at least once) reaches a maximum of $\sim$80% for the $\tilde{\tau}\tilde{\tau}$ channel and >90% for other channels at a slepton decay length of around 10 cm. An efficiency >10% is maintained for slepton decay lengths from $\sim$1 mm to $\sim$10 m for all channels.

The numbers of background events expected to be selected in at least one topology and the corresponding numbers of observed events for each LEP energy and each selection are given in Table 4. The efficiency dependence on the slepton decay length is shown in Fig. 3b, for the prompt decay and the short and long decay length selections.

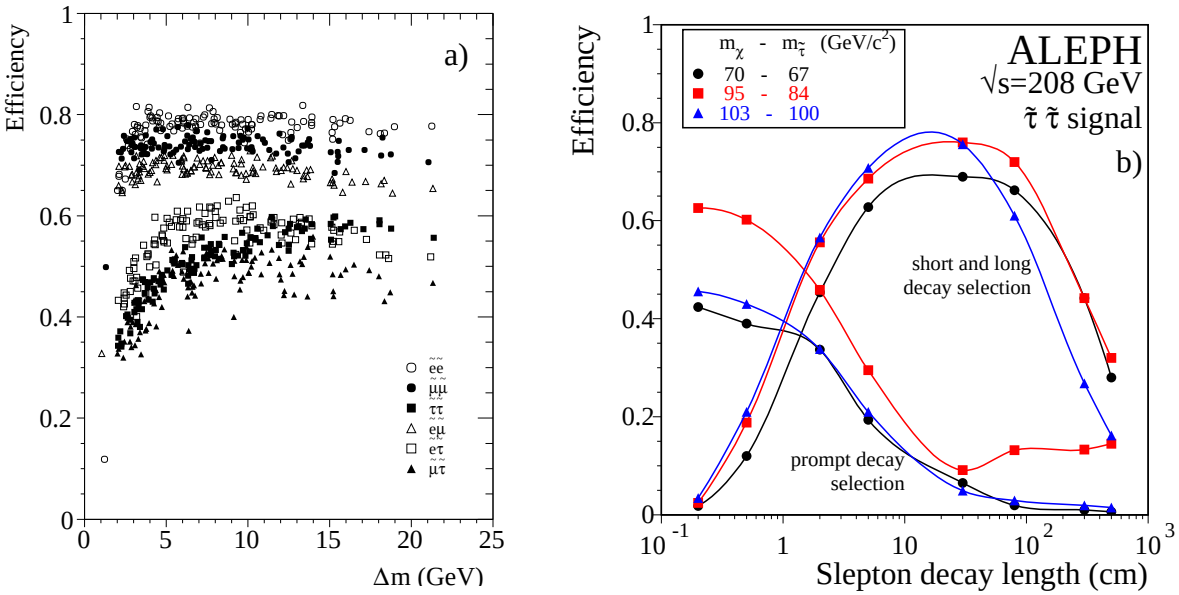

Figure 3: a) Selection efficiencies for the six different event topologies versus $\Delta m = m_{\chi}$-$m_{\tilde{\ell}}$ in the zero slepton lifetime case. The spread of points observed for a given topology is due to different values of neutralino and slepton masses. b) Probability for a signal stau-pair event to be selected by at least one of the six topological searches versus slepton decay length. The set of curves with higher efficiency in the 0.1 cm area corresponds to the prompt decay selection. Those peaking at ∼10 cm correspond to the short and long decay length selection. Different lines correspond to different points in the (m_{χ},$m_{\tilde{\tau}}$) space.

4 Interpretation of the results in the minimal GMSB model

A scan over the parameters of a minimal GMSB model has been performed to study the impact of the different searches. The aim of this scan is to understand which topologies contribute to exclude regions in the parameter space and to be able to set a lower limit on the mass of the NLSP and on the universal mass scale Λ, independently of the NLSP lifetime (i.e., for all gravitino masses).

The parameters needed to specify a minimal GMSB model [1] are

- Λ, the universal mass scale of SUSY particles;
- N_5, the number of messenger pairs;
- $M_{\rm mess}$, the common messenger mass scale;
- $\tan\beta$, the ratio between the vacuum expectation values of the two Higgs doublets;

Table 5: Minimal set of parameters and their ranges of variation in the scan.

Parameter	Lower limit	Upper limit
$M_{\rm mess}$	10^4 GeV	10^{12} GeV
$m_{\tilde{\rm G}}$	10^{-1} eV	10^5 eV
Λ	10^3 GeV	$\min(\sqrt{F}, M_{\rm mess})$
$\tan\beta$	1.5	40
N_5	1	5
sign(μ)	$-$	$+$

- sign(μ), where μ is the higgsino mass parameter; and
- $\sqrt{F}$, the SUSY breaking scale in the messenger sector, related to the gravitino mass by

$$m_{\tilde{\rm G}} = \frac{F}{\sqrt{3}\ M_{\rm Planck}} = 2.4 \left(\frac{\sqrt{F}}{100\,{\rm TeV}} \right)^2 \ {\rm eV}, \tag{2}$$

where $M_{\rm Planck} = 2.4 \times 10^{18}\,{\rm GeV}/c^2$ is the reduced Planck mass.

The ranges of the scan are listed in Table 5. The six parameters listed determine the properties of supersymmetric particles characteristic of GMSB models. At each point in the scan, the `ISAJET 7.51` program [18] was used to calculate SUSY masses, cross sections, branching ratios and lifetimes, then taken into account to evaluate whether a point is excluded by any of the searches. In total, over 2.3 million points in the minimal GMSB parameter space have been tested.

In addition to the analyses described in this paper, other searches were used to set exclusion areas in the scan: the SUGRA chargino [17] and slepton [13] searches to cover the case of χ NLSP with a long-lived neutralino and LEP1 results [19, 20], used here to exclude very low NLSP masses. In addition, for each set of GMSB parameters the Higgs boson masses and couplings were computed. The results from Ref. [21] were used to extend the GMSB exclusion domain.

4.1 Lower limit on the NLSP mass

As reported in Section 3, no significant deviation from the SM expectation was observed. A lower limit on the $\tilde{\tau}_1$ mass of $77\,{\rm GeV}/c^2$ is set, independently of its lifetime. This limit is valid in the stau NLSP case over the full scan range. It is reduced to $72\,{\rm GeV}/c^2$ in the χ NLSP scenario.

The interplay of the different searches in the $(m_\chi, m_{\tilde{\tau}})$ plane is shown in Fig. 4. For short NLSP lifetimes (Fig. 4a) the multi-lepton search is able to exclude m_χ up to $92\,{\rm GeV}/c^2$ in the slepton NLSP case, extending the acoplanar lepton search. In Fig. 4b the case of long NLSP lifetimes is presented. Because they rely on results from indirect constraints, limits in the long neutralino lifetime case are less constraining than those obtained with short neutralino

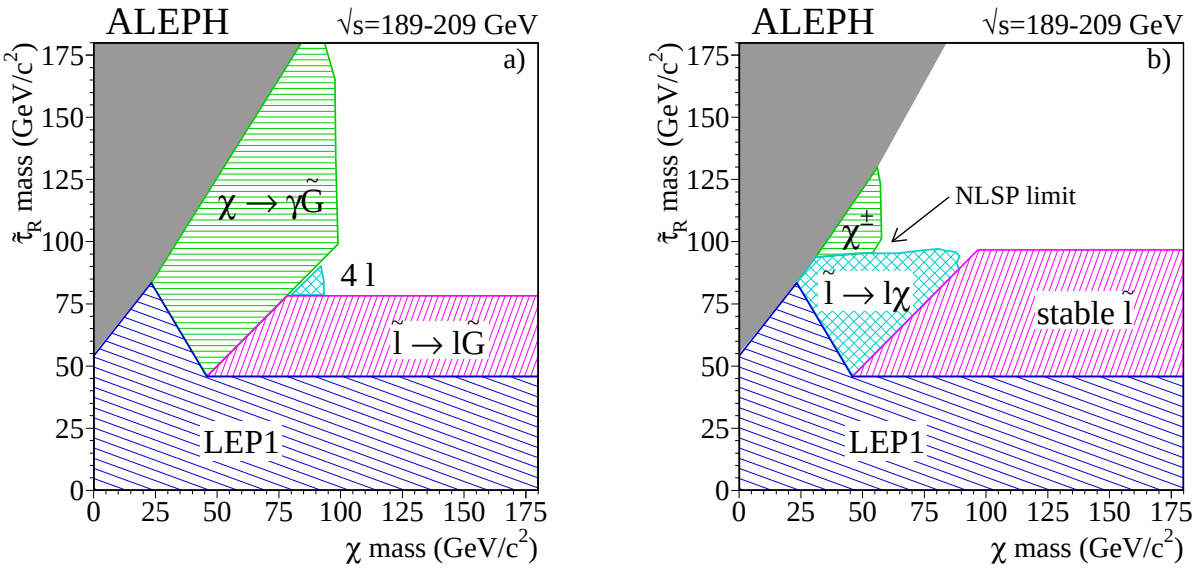

Figure 4: Regions excluded by the different analyses described in the text at 95% confidence level in the $(m_\chi, m_{\tilde{\tau}})$ plane, for a) short NLSP lifetimes ($m_{\tilde{\mathrm{G}}} \leq 10\,\mathrm{eV}/c^2$) and b) long NLSP lifetimes ($m_{\tilde{\mathrm{G}}} \geq 1\,\mathrm{keV}/c^2$). Points in the dark region are not accessible to the scan. The absolute NLSP mass limit is set at $54\,\mathrm{GeV}/c^2$ in b) by the intersection of chargino and slepton searches.

lifetime searches. The absolute lower limit on the NLSP mass of $54\,\mathrm{GeV}/c^2$, determined by the chargino and slepton searches, is visible in Fig. 4b. This point is found at $N_5 = 1$, $\tan\beta = 3$, $\Lambda = 39\,\mathrm{TeV}/c^2$, $M_{\mathrm{mess}} = 10^{10}\,\mathrm{GeV}/c^2$ and $m_{\tilde{\mathrm{G}}} = 10^5\,\mathrm{eV}/c^2$, where the neutralino is the NLSP with the $\tilde{\ell}$ masses around $96\,\mathrm{GeV}/c^2$ and all other supersymmetric particles above threshold.

The impact of the neutral Higgs boson searches on the neutralino and stau mass limits is shown in Fig. 5 as a function of $\tan\beta$. The NLSP absolute mass limit is $77\,\mathrm{GeV}/c^2$ obtained for large $\tan\beta$ and in the stau NLSP scenario.

4.2 Lower limit on Λ

The parameter Λ represents the energy scale at which the messenger particles couple to the visible sector and hence fixes the universal mass scale of SUSY particles. At the M_{mess} energy, gaugino masses scale like $N_5\Lambda$, while scalar masses squared scale like $N_5\Lambda^2$. The masses at the electroweak scale are calculated by means of the renormalization group equations. Once the limit for the NLSP mass has been found, the limit on Λ as a function of N_5 can thus be derived.

The excluded values for the parameter Λ as a function of $\tan\beta$ are shown in Fig. 6 for different values of N_5. The absolute limit for Λ is set at around $10\,\mathrm{TeV}/c^2$. This limit is set at $N_5 = 5$, $\tan\beta = 1.5$, $M_{\mathrm{mess}} = 10^{12}\,\mathrm{GeV}/c^2$ and a large gravitino mass (stable NLSP). The neutralino is the NLSP with a mass of $73\,\mathrm{GeV}/c^2$, slepton masses are around $76\,\mathrm{GeV}/c^2$ and all other sparticles are above threshold.

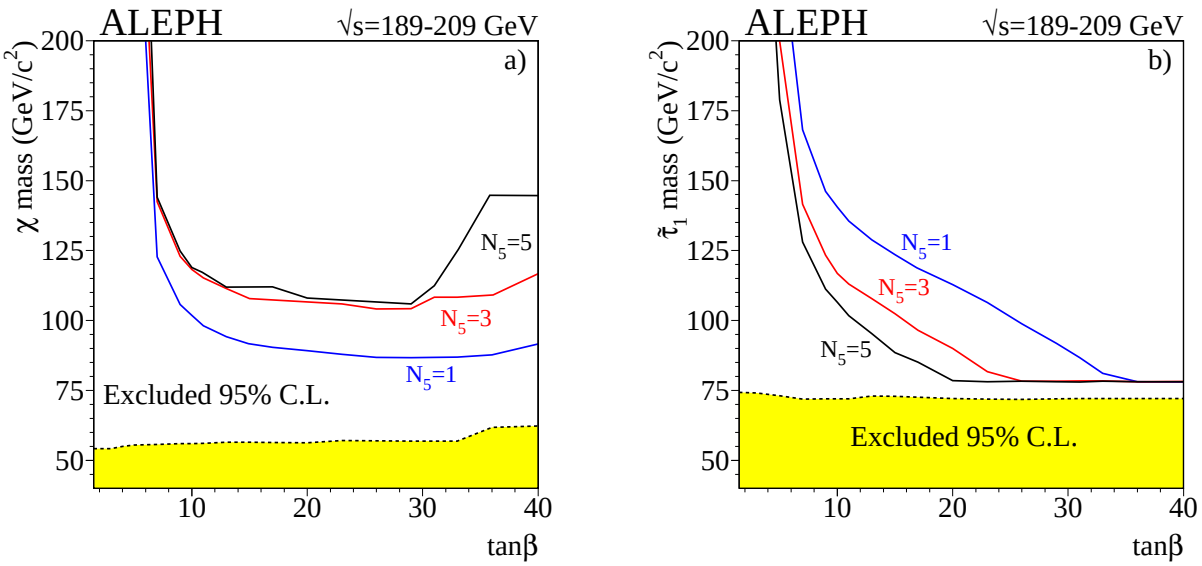

Figure 5: Lower limits on the masses of a) χ and b) $\tilde{\tau}_1$ as a function of $\tan\beta$, for different values of N_5, as set by the Higgs boson searches. The shaded area represents the minimum excluded area, for any N_5, as derived from GMSB searches alone.

The impact of the neutral Higgs boson searches [21] is shown in the $(\Lambda, \tan\beta)$ plane in Fig. 6d. These results strongly constrain the allowed values of Λ for small $\tan\beta$. For example, for $N_5 = 1$, Λ up to $67\,\mathrm{TeV}/c^2$ and $\tan\beta$ up to 6 are excluded.

The lower limit on Λ independent of lifetime and $\tan\beta$ is shown in Fig. 7a as a function of N_5. The absolute limit of $\Lambda > 10\,\mathrm{TeV}/c^2$ can be seen here for $N_5 = 5$. When the Higgs boson search results are taken into account, the limit on Λ increases to $16\,\mathrm{TeV}/c^2$, for $m_t = 175\,\mathrm{GeV}/c^2$. With a top mass of $180\,\mathrm{GeV}/c^2$, the absolute lower limit on Λ is set at $15\,\mathrm{TeV}/c^2$.

The equation that relates the gravitino mass to the scale of SUSY breaking in the messenger sector, $m_{\tilde{G}} = F/\sqrt{3}M_{\mathrm{Planck}}$, can be exploited to put an indirect limit on the gravitino mass. The universal mass scale must obey $\Lambda \leq \sqrt{F}$ under the simple assumption of positive messenger masses squared [1]. The lower limit on Λ can then be converted into a constraint on $\sqrt{F}$ and therefore provides an indirect limit on the gravitino mass. The dependence of $m_{\tilde{G}}$ on N_5 is illustrated in Fig. 7b. The lower limit on Λ of $10\,\mathrm{TeV}/c^2$ implies a lower limit on $m_{\tilde{G}}$ of $0.024\,\mathrm{eV}/c^2$. When the results of Higgs searches are included these limits become $16\,\mathrm{TeV}/c^2$ and $0.061\,\mathrm{eV}/c^2$, respectively.

5 Conclusions

No evidence for new physics has been found in the search for GMSB topologies in the final ALEPH data sample collected at $\sqrt{s}$ up to 209 GeV. In order to test the impact of the searches reported here and in Refs. [13, 17, 21], a scan over a minimal set of GMSB parameters has been

Table 6: NLSP mass limits, as derived from the scan

NLSP	mass limit (95% C.L.)	validity
χ	92 GeV/c^2	short χ lifetime
	54 GeV/c^2	any lifetime
$\tilde{\tau}_1$	77 GeV/c^2	any lifetime
any	77 GeV/c^2	Higgs exclusion

performed. The resulting NLSP mass limits can be read in Table 6.

The scan also provides a lower limit of 16 TeV/c^2 on the universal SUSY mass scale Λ and an indirect lower limit on the gravitino mass of 0.061 eV/c^2.

Acknowledgements

It is a pleasure to congratulate our colleagues from the accelerator divisions for the successful operation of LEP at high energy. We are indebted to the engineers and technicians in all our institutions for their contribution to the excellent performance of ALEPH. Those of us from non-member states wish to thank CERN for its hospitality and support.

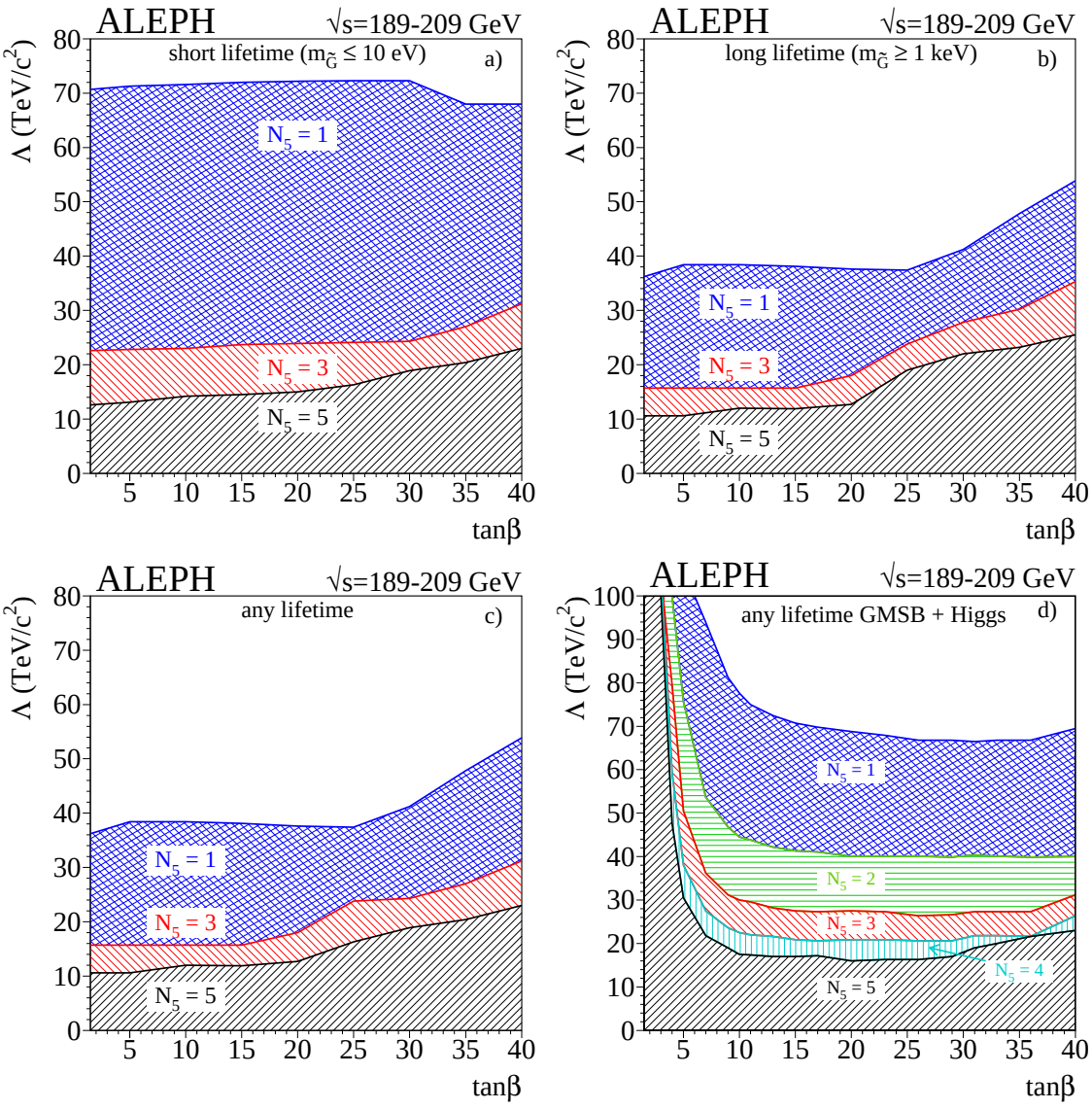

Figure 6: Region excluded at 95% C.L. in the $(\Lambda, \tan\beta)$ plane for a) short, b) long and c) any NLSP lifetime. The impact of the Higgs search is included in d). Values of $\tan\beta$ less than 3 are excluded for large N_5 at any mass parameter Λ, while $\tan\beta$ up to 6 can be excluded for $N_5 = 1$.

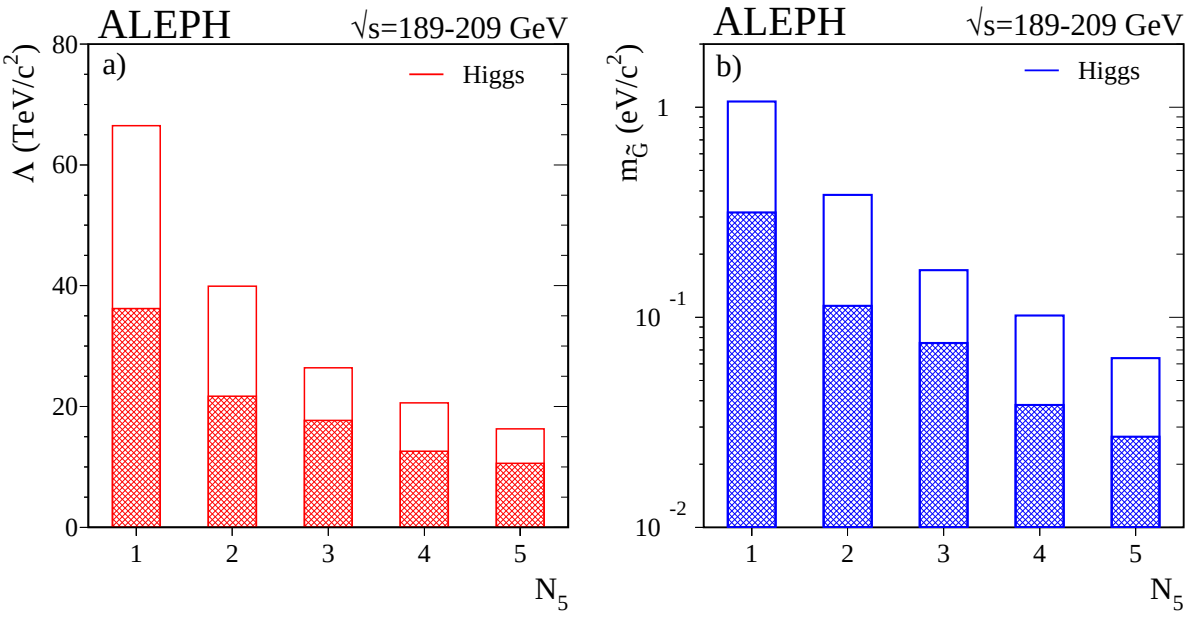

Figure 7: Exclusions at 95% confidence level (a) for Λ and (b) for $m_{\tilde{\mathrm{G}}}$ as a function of N_5, derived from the minimal GMSB scan (shaded). The unshaded bars represent the excluded region when the neutral Higgs boson exclusion is applied with $m_{\mathrm{t}} = 175\,\mathrm{GeV}/c^2$.

Appendix A: Four leptons with negligible lifetime selection

The experimental topology consists of two energetic (from the $\tilde{\ell} \to \ell\tilde{G}$ decay) and two soft (from the $\chi \to \ell\tilde{\ell}$ decay) leptons plus missing energy and momentum. The charge of the two most energetic leptons is expected to be the same in 50% of the cases.

In the analysis the presence of at least two energetic leptons is required, where, in the case of tau decays, a lepton can also be a jet with small multiplicity and invariant mass. The same muon, electron and tau identification as described in [6] is applied.

All topologies have a common anti–$\gamma\gamma$ preselection, based on the rejection of events with low transverse momentum or with energy deposits at small polar angles, which indicate the presence of a scattered electron. The anti–$\gamma\gamma$ cuts include:

- $p_\perp/\sqrt{s} > 0.075$ or ($p_\perp/\sqrt{s} > 0.05$ and $|\phi_{\rm miss} - 90^\circ| > 15^\circ$ and $|\phi_{\rm miss} - 270^\circ| > 15^\circ$);
- $\theta_{\rm diff} > 5^\circ$ or $\theta_{\rm scatt} > 15^\circ$;
- $E_{\rm nh}/E_{\rm tot} < 0.45$ and ($E_{\rm nh}/E_{\rm tot} < 0.30$ or $p_{\perp{\rm nnh}}/\sqrt{s} > 0.03$);
- $\cos\theta_{\rm miss} < 0.95$

The cut variables are defined as follows: $p_\perp$ is the transverse momentum of the event, $\phi_{\rm miss}$ and $\theta_{\rm miss}$ are the azimuthal and polar angles of the missing momentum, $\theta_{\rm diff}$ and $\theta_{\rm scatt}$ are two angles associated with the $\gamma\gamma$ kinematic hypothesis described in Ref. [22], $E_{\rm nh}$ is the reconstructed neutral–hadron energy, $E_{\rm tot}$ is the total reconstructed energy of the event and $p_{\perp{\rm nnh}}$ is the transverse momentum of the event evaluated without the neutral hadrons.

A.1 $\tilde{\rm e}\tilde{\rm e}$, $\tilde{\mu}\tilde{\mu}$, $\tilde{\rm e}\tilde{\mu}$ selections

Events with 2, 3 or 4 charged tracks are considered in the case of topologies that do not involve tau leptons in the final state. At least three identified electrons (muons) are required in the $\tilde{\rm e}\tilde{\rm e}$ ($\tilde{\mu}\tilde{\mu}$) selections. In the $\tilde{\rm e}\tilde{\mu}$ selection the number of identified leptons must again be at least three, but the two most energetic leptons must have different flavours and no more than two leptons of the same flavour are allowed. These requirements reject most hadronic background decays. After the preselection, the cuts listed in Table 7 are applied to reject planar events and improve the $\gamma\gamma$ suppression. If the two most energetic leptons have different charges, further selections are necessary to reduce the remaining WW and ZZ background, and in the case of $\tilde{\rm e}\tilde{\rm e}$, the Bhabha background.

The cut variables are defined as follows: E_{30} is the total energy reconstructed in a 30° cone around the beam line, AcopT [19] is the transverse acoplanarity of the two most energetic leptons, $\ell 1$ and $\ell 2$. Acol is the angle between $\ell 1$ and $\ell 2$ in space and $E_{\ell 1}$ is the energy of the most energetic lepton in the event. In the $\tilde{\rm e}\tilde{\rm e}$ case, an event is accepted if either the cut on the energy of the second most energetic lepton, $E_{\ell 2}$, or a veto on isolated photons, $\gamma_{\rm iso}$, is satisfied. $E_{\rm lt}$ is the energy of the leading track in the event.

Table 7: Selection cuts applied to the $\tilde{e}\tilde{e}$, $\tilde{\mu}\tilde{\mu}$ and $\tilde{e}\tilde{\mu}$ topologies.

Variable	$\tilde{e}\tilde{e}$	$\tilde{\mu}\tilde{\mu}$	$\tilde{e}\tilde{\mu}$
$E_{30}/\sqrt{s}$	< 0.12	< 0.12	< 0.12
AcopT	$< 175^\circ$	$< 175^\circ$	$< 175^\circ$
Acol	$< 176^\circ$	-	-
$E_{\ell 1}/\sqrt{s}$	< 0.37	-	-
if Charge($\ell 1$) $\neq$ Charge($\ell 2$)			
$E_{\ell 1}/\sqrt{s}$	< 0.39	< 0.40	< 0.39
$E_{\ell 2}/\sqrt{s}$	< 0.33 } or	-	-
$\gamma_{\rm iso}$	veto }	-	-
Acol	-	-	$< 172^\circ$
$E_{\rm lt}/\sqrt{s}$	-	-	> 0.12 and < 0.37

A.2 $\tilde{e}\tilde{\tau}$, $\tilde{\mu}\tilde{\tau}$, $\tilde{\tau}\tilde{\tau}$ selections

The selection procedures for the $\tilde{e}\tilde{\tau}$ and $\tilde{\mu}\tilde{\tau}$ topologies are based on the acoplanar leptons analysis developed in Ref. [6] where a detailed definition of the tau reconstruction algorithm is also given. The selection cuts for mixed topologies are listed in Table 8.

Table 8: Selection cuts applied to the $\tilde{e}\tilde{\tau}$ and $\tilde{\mu}\tilde{\tau}$ topologies.

Variable	$\tilde{e}\tilde{\tau}$	$\tilde{\mu}\tilde{\tau}$
N(charged)	$= (4, 5, 6)$	$= (4, 5, 6)$
$N(\ell = \mu$ or e)	$N(\mathrm{e}) \geq 1$	$N(\mu) \geq 1$
N_τ	≥ 2	≥ 2
$M_{\rm tot}/\sqrt{s}$	> 0.06 and < 0.6	> 0.06 and < 0.6
Acol	$< 175^\circ$	$< 175^\circ$
$E_{12}/\sqrt{s}$	< 0.02	< 0.02
Thrust	< 0.96	< 0.96
$M_{\rm miss}/\sqrt{s}$	> 0.1 and < 0.8	> 0.1 and < 0.8
$M(\mathrm{Event} - \tau 1)/\sqrt{s}$	< 0.54	< 0.55
$E_{\tau 1}/\sqrt{s}$	> 0.17 and < 0.38	> 0.14 and < 0.36
$E_{\tau 2}/\sqrt{s}$	> 0.01 and < 0.26	> 0.01 and < 0.30
$M_{\tau 1}/\sqrt{s}$	> 0.04 and < 0.25	> 0.02 and < 0.25
$M_{\tau 2}/\sqrt{s}$	< 0.17	< 0.18
$E_{\ell 1}/\sqrt{s}$	> 0.14 and < 0.36	> 0.12 and < 0.36
$E_{\ell 2}/\sqrt{s}$	< 0.24	< 0.28
$N_{\rm nh}(\tau 1)$	-	< 2

The definition of the variables used is the following: N(charged) is the number of reconstructed charged tracks, $N(\ell)$ is the number of identified leptons (ℓ = e, μ), $M_{\rm tot}$ is the invariant mass of the event, Acol is the acollinearity of the two tau jets, E_{12} is the total energy reconstructed in a 12° cone around the beam line, $M_{\rm miss}$ is the missing mass of the event, $M(\mathrm{Event} - \tau 1)$ is the invariant mass of the event once the most energetic tau jet, $\tau 1$, has been

removed, $E_{\tau 1}$ and $E_{\tau 2}$ are the energies of the two tau jets, $M_{\tau 1}$ and $M_{\tau 2}$ are the corresponding masses. $N_{\rm nh}(\tau 1)$ is the number of neutral hadrons reconstructed in the most energetic tau jet.

The cuts on $M_{\rm tot}$ and E_{12} allow further $\gamma\gamma$ suppression while the cuts on N(charged), $N(\ell)$ and $N_{\rm nh}(\tau 1)$ reject most of the $q\bar{q}$ background and hadronic decays. The kinematic cuts on the jet variables select events containing tau-like jets.

For the $\tilde{\tau}\tilde{\tau}$ topology the events are clustered into four jets using the Durham algorithm [23] and each jet is checked for consistency with a tau hypothesis. Events satisfying the cuts listed in Table 9 are retained. Two alternative strategies are applied depending on wether the sum of the charges of the tracks in the two most–energetic tau jets is zero, Charge(jet1 + jet2) = 0, or Charge(jet1 + jet2) = 1 or 2.

Table 9: Selection cuts applied to the $\tilde{\tau}\tilde{\tau}$ topology.

Variable	$\tilde{\tau}\tilde{\tau}$	
$-\ln y_{23}$	> 2 and < 8.5	
$-\ln y_{34}$	< 9.5	
$-\ln y_{45}$	< 11	
$N_{\rm good}$	> 2 and < 9	
$N_{\rm cj}$	≥ 3	
$N(\tau)$	≥ 3	
$N_{\rm cnt}$	≤ 2	
$M_{\rm tot}/\sqrt{s}$	> 0.06 and < 0.5	
$E_{12}/\sqrt{s}$	< 0.05	
$E_{30}/\sqrt{s}$	< 0.09	
AcopT	$< 178^\circ$	
$E_{\tau_{\rm max}}/\sqrt{s}$	< 0.3	
$M_{\rm miss}/\sqrt{s}$	> 0.3 and < 0.9	
Charge(jet1 + jet2)	$= 0$	$= 1, 2$
Thrust	< 0.96	< 0.98
Acop	$< 172^\circ$	$< 171^\circ$
$p_{\ell_{\rm max}}/\sqrt{s}$	< 0.23	< 0.26

The cut variables are defined as follows: y_{23} (y_{34}, y_{45}) is the y cut for which the event goes from 2 to 3 (3 to 4, 4 to 5) jets. $N_{\rm good}$ is the number of good tracks, $N_{\rm cj}$ is the number of jets containing at least one charged track, $N(\tau)$ is the number of identified tau jets, $N_{\rm cnt}$ is the number of charged tracks not associated with any tau jet. $E_{\tau_{\rm max}}$ is the energy of the most energetic tau jet in the event. $p_{\ell_{\rm max}}$ is the momentum of the most energetic identified lepton (e or μ) from the most energetic tau jet (including final state radiation).

The cuts have been optimised to select events with at least three tau-like jets not lying in the same plane. They reject most Standard Model processes leaving an irreducible contribution arising from WW and $\tau\tau(\gamma)$ events.

Appendix B: Four leptons with lifetime selection

In analogy with the negligible lifetime analysis, described in Appendix A, six selections corresponding to the six different final states have been developed.

The main requirement for selection is that an event has at least one *high-d_0* track. The main background to such an object is given by secondary interactions of particles originating from SM processes with the detector material (e.g. nuclear interactions, photon conversions, etc). The rejection of this background is achieved through detailed analysis of the TPC, ITC and VDET hits associated to the reconstructed high-d_0 tracks. Three variables are used to select a high-d_0 track: the momentum, the d_0 and $\chi^2_{\rm IP}$ (the χ^2 of the track fit to the interaction point, normalised to the number of degrees of freedom). The d_0 cut is not applied if the track $|z_0|$ is greater than 8 cm. For each topology two sets of cuts have been applied to cope with the two cases of short slepton decay length ($d_{\tilde{\ell}} \sim 1$ cm) and of long slepton decay length ($d_{\tilde{\ell}} \sim 1$ m). These cuts are summarised in Table 10. For the $\tilde{\rm e}\tilde{\rm e}$, $\tilde{\mu}\tilde{\mu}$ and $\tilde{\rm e}\tilde{\mu}$ channels the electron and/or muon identification is also applied to the high-d_0 track.

Table 10: The cuts on track momentum (p), d_0 and $\chi^2_{\rm IP}$ for each channel under each selection. A track must have parameters greater than these values to be considered as a good high-d_0 track in the corresponding selection.

Variable	Selection	$\tilde{\rm e}\tilde{\rm e}$	$\tilde{\mu}\tilde{\mu}$	$\tilde{\tau}\tilde{\tau}$	$\tilde{\rm e}\tilde{\mu}$	$\tilde{\rm e}\tilde{\tau}$	$\tilde{\mu}\tilde{\tau}$
p (GeV)	low $d_{\tilde{\ell}}$	19.0	20.0	4.7	14.9	10.0	8.1
	high $d_{\tilde{\ell}}$	19.8	18.6	6.1	20.0	8.5	4.3
d_0 (cm)	low $d_{\tilde{\ell}}$	0.17	0.50	0.20	0.20	0.24	0.50
	high $d_{\tilde{\ell}}$	0.50	0.50	0.50	0.50	0.49	0.48
$\chi^2_{\rm IP}$	low $d_{\tilde{\ell}}$	700	550	230	180	210	700
	high $d_{\tilde{\ell}}$	680	690	700	700	590	610

In addition to the request of having at least one high-d_0 track, an event is also required to pass at least one of six selections based on global event variables. The principal cuts are listed in Table 11.

Most analyses use only tracks with a d_0 less than 2 cm and a $|z_0|$ less than 10 cm, and ignore all others. Some of the variables, indicated as primed, are calculated using only tracks with these d_0 and $|z_0|$ conditions, while unprimed variables are calculated using all tracks. The definitions of the variables are as follows: $N_{\rm ch}$ is the number of charged tracks, $N_{\rm TPC}$ is the number of charged tracks with at least one TPC hit, $E_{\rm tot}$ is the total energy of the event, $m_{\rm tot}$ is the invariant mass of the event, α is the acollinearity of the event, c_{2ch} is cosine of the angle between the two highest momentum tracks, $S'_{2\beta}$ is $\sqrt{1-0.5(\beta_1^2+\beta_2^2)}$ (where β_1 and β_2 are the boosts of the two event hemispheres) and $\Phi_{\rm aco}$ is the acollinearity of the event.

The cuts marked with a † are not applied if a parent slepton track has been identified (i.e. a mother-daughter relationship has been established between one of the high-d_0 tracks and a track from the primary interaction point). The cuts on c_{2ch}, $S'_{2\beta}$ and $\Phi'_{\rm aco}$ are only applied in the case that there is just one good high-d_0 track, and that no track or hit has been tagged as belonging to its parent slepton. Only one of the cuts grouped with a brace need to be passed.

Table 11: Global event variable cuts.

Variable	$\tilde{e}\tilde{e}$, $\tilde{\mu}\tilde{\mu}$, $\tilde{e}\tilde{\mu}$	$\tilde{e}\tilde{\tau}$, $\tilde{\mu}\tilde{\tau}$	$\tilde{\tau}\tilde{\tau}$
$N_{\rm ch}$	>2 and <20	>2	–
$N'_{\rm ch}$	>7	<9	–
$N_{\rm TPC}$	–	<12	>2 and <14
$N'_{\rm TPC}$	–	<10	<11
$E'_{\rm tot}$	–	>6 GeV †	>6 GeV and $<0.75\sqrt{s}$
$m'_{\rm tot}$	–	>7.7 GeV †	>7.7 GeV
α'	–	<178° †	<178°
c_{2ch}	>-0.999 and <0.99	>-0.999 and <0.99	>-0.999 and <0.99
$S'_{2\beta}$	>0.1 } or	>0.1 } or	>0.2 } or
$\Phi'_{\rm aco}$	<174° }	<174° }	<174° }

In addition, cosmic-ray events are suppressed by requiring that the event be within 100 ns of the bunch crossing.

References

[1] For a review see:

G.F. Giudice and R. Rattazzi, *Theories with gauge-mediated supersymmetry breaking,* Phys. Rept. **322** (1999) 419;
S. Ambrosanio, G.D. Kribs and S.P. Martin, *Signals for gauge-mediated supersymmetry breaking models at the CERN LEP2 collider,* Phys. Rev. **D56** (1997) 1761.

[2] H.P. Nilles, *Supersymmetry, supergravity and particle physics,* Phys. Rep. **110** (1984) 1.

[3] A. De Gouvêa, T. Moroi and H. Murayama, *Cosmology of supersymmetric models with low-energy gauge mediation,* Phys. Rev. **D56** (1997) 1281.

[4] ALEPH Collaboration, *Searches for supersymmetry in the photon(s) plus missing energy channel at a centre–of–mass energy of 161 and 172 GeV,* Phys. Lett. **B420** (1998) 127;
ALEPH Collaboration, *A study of single– and multi–photon production in e^+e^- collisions at a centre–of–mass energy of 183 GeV,* Phys. Lett. **B427** (1998) 201.

[5] ALEPH Collaboration, *Search for pair-production of long-lived heavy charged particles in e^+e^- annihilation,* Phys. Lett. **B405** (1997) 379;
ALEPH Collaboration, *Search for sleptons in e^+e^- collisions at centre–of–mass energies up to 161 and 172 GeV,* Phys. Lett. **B407** (1997) 377.

[6] ALEPH Collaboration, *Search for sleptons in e^+e^- collisions at centre–of–mass energies up to 184 GeV,* Phys. Lett. **B433** (1998) 176.

[7] ALEPH Collaboration, *Search for gauge mediated SUSY breaking topologies at $\sqrt{s} \sim 189$ GeV,* Eur. Phys. J. **C16** (2000) 71.

[8] DELPHI Collaboration, *Search for supersymmetric particles in scenarios with a gravitino LSP and stau NLSP,* Eur. Phys. J. **C16** (2000) 211.

[9] OPAL Collaboration, *Searches for prompt light gravitino signatures in e^+e^- collisions at $\sqrt{s} = 189$ GeV,* Phys. Lett. **B501** (2000) 12.

[10] CDF Collaboration, *Limits on gravitino production and new processes with large missing transverse energy in p anti-p collisions at $\sqrt{s} = 1.8$ TeV,* Phys. Rev. Lett. **85** (2000) 1378;
D0 Collaboration, *Experimental search for chargino and neutralino production in supersymmetry models with a light gravitino.* Phys. Rev. Lett. **80** (1998) 442.

[11] ALEPH Collaboration, *ALEPH: A detector for electron–positron annihilations at LEP,* Nucl. Instrum. Methods **A294** (1990) 121.

[12] ALEPH Collaboration, *Performance of the ALEPH detector at LEP,* Nucl. Instrum. Methods **A360** (1995) 481.

[13] ALEPH Collaboration, *Search for scalar leptons in e^+e^- collisions at centre-of-mass energies up to 209 GeV,* CERN EP/2001-086. To appear in Phys. Lett. B.

[14] ALEPH Collaboration, *Single- and multi-photon production in e^+e^- collisions at centre-of-mass energies between 189 and 207 GeV,* contribution # 232 to the IECHEP, Budapest, Hungary, 12–18 July 2001, ALEPH-CONF 2001-007. Paper in preparation.

[15] S. Katsanevas and P. Morawitz, *SUSYGEN-2.2: A Monte Carlo event generator for MSSM sparticle production at e^+e^- colliders,* Comput. Phys. Commun. **12** (1998) 227.

[16] J.-F. Grivaz and F. Le Diberder, *Complementary analyses and acceptance optimization in new particles searches,* LAL preprint # 92–37 (1992);
ALEPH Collaboration, *Search for the standard model Higgs boson,* Phys. Lett. **B313** (1993) 299.

[17] ALEPH Collaboration, *Search for charginos and neutralinos in e^+e^- collisions at $\sqrt{s}$ up to 208 GeV and mass limit for the lightest neutralino,* contribution # 233 to the IECHEP, Budapest, Hungary, 12–18 July 2001, ALEPH-CONF 2001-047. Paper in preparation.

[18] H. Baer, F.E. Paige and S.D. Protopopescu, *ISAJET 7.48: A Monte Carlo event generator for pp, $\bar{p}p$, and e^+e^- reactions,* hep-ph/0001086, (`http://paige.home.cern.ch/paige/`).

[19] ALEPH Collaboration, *Searches for new particles in Z decays using the ALEPH detector,* Phys. Rep. **216** (1992) 253.

[20] The LEP Collaborations, *A combination of preliminary electroweak measurements and constraints on the Standard Model,* CERN EP/99-015.

[21] ALEPH Collaboration, *Final results of the ALEPH searches for neutral Higgs bosons,* CERN EP/2001-095. To appear in Phys. Lett. B.

[22] ALEPH Collaboration, *Searches for scalar top and scalar bottom quarks at LEP2,* Phys. Lett. **B413** (1997) 431.

[23] Yu.L. Dokshitzer, J. Phys. **G17** (1991) 1481.